

# High Temperature Creep Properties of Sn-3.5Ag and Sn-5Sb Lead-free Solder Alloys

SHIMODA Masayoshi \*, HIDAHA Noboru\*\*, WATANABE Hirohiko \*\*\* and YOSHIBA Masayuki \*\*\*\*

## Abstract

*In order to acquire relevant creep characteristics such as stress exponent and activation energy, creep strain tests were conducted on Sn-3.5Ag and Sn-5Sb systems of solder alloys in the intermediate temperature regime from 353 K to 453 K corresponding to the homologous temperatures  $\eta=0.715\sim0.917$  and  $\eta=0.699\sim0.897$  for the two alloys, respectively. It was found that an apparent creep-activation energy of both Sn-3.5Ag and Sn-5Sb solder alloys had a change point at  $\eta=0.82$  under the higher stress of 9.8 MPa. At the lower stress of 4 MPa, the change point was found only for Sn-5Sb alloy. Moreover, under the lower stress level, the stress exponent of both solder alloys are approximately 1, while under the higher stress region (more than 9.8 MPa), the stress exponents of both solders are 7 or more. Determining factors of creep deformation are discussed in relation to the temperature and stress region. It was considered that the deformation of both solder alloys is dominated by the rate of the dislocation climb/dislocation glide in the higher temperature and stress region.*

**KEY WORDS:** (Lead-free solder alloys), (Creep), (Activation energy), (Dislocation)

## 1. Introduction

As part of efforts to protect the global environment, strict regulations on the use of lead (Pb) for soldering are applied in electrical and electronic equipment, as well as other hazardous substances in Japan, in accordance with the RoHS Directive which took effect in the EU in July 2006. On the other hand, heat generation in electronic components and soldering tends to increase remarkably in high density packaging. In particular, because electronic equipment for industrial and automotive applications, as represented by power devices, is used under severe environments characterized by large applied current, vibration, etc., the strength properties of Pb-free solders used to joining parts have a large effect on the durability and reliability of those parts.

In earlier research, the authors studied a series of materials in which trace elements (Ge, Ni) were added to Sn-Ag-Cu solders, focusing on wettability and durability against thermal fatigue, and demonstrated, for example, that addition of an appropriate amount of Ge is effective in reducing oxide dross<sup>1)</sup>, while Ni is effective in suppressing the growth of an intermetallic compound phase at bonded interfaces<sup>2)</sup> and improving creep properties by suppressing coarsening of the SnCu compound phase<sup>3,4)</sup>. Creep properties are generally

considered to be determined as follows. (1)the intrinsic strength of the base metal, (2)solid-solution strengthening by addition of solution elements, and (3) precipitation strengthening by the precipitation reaction with added elements, etc.

Accordingly, investigation of the effect of the main strengthening mechanisms of solder alloys on high temperature creep behavior is fundamentally important. From this viewpoint, in the present research, we investigated creep behavior of the high temperature region for Sn-5Sb solder alloy as a representative example of a solid solution alloy, in which solution strengthening is the main strengthening mechanism, and Sn-3.5Ag solder alloy as a representative example of an alloy in which precipitation strengthening is expected.

The creep properties of these two types of solder alloys have already been investigated by Nishida et al. using the nano-indentation method, and important knowledge was obtained<sup>5)</sup>. However, with the nano-indentation method, there is a high possibility of remarkable changes in creep properties, as the results are strongly dependent on the microstructure around the indentation, and for practical application to power devices, etc., an accurate grasp of the macro creep deformation behavior of solder alloys over a wide region

† Received on December 26, 2011

\* Specially Appointed Assistant Professor

\*\* Guest Academic Staff (Fuji Electric Co.,Ltd.)

\*\*\* Guest Researcher (Fuji Electric Co.,Ltd.)

\*\*\*\* Graduate School of Science and Engineering Tokyo Metropolitan University

Transactions of JWRI is published by Joining and Welding Research Institute, Osaka University, Ibaraki, Osaka 567-0047, Japan

## High Temperature Creep Properties of Sn-3.5Ag and Sn-5Sb Lead-free Solder Alloys

of the bulk becomes important. Thus, it must inevitably be said that it is difficult to obtain the necessary understanding by the nano-indentation method.

From this viewpoint, in this research, the temperature dependence and stress dependence of high temperature creep in the above-mentioned Sn-3.5Ag solder alloy and Sn-5Sb solder alloy were investigated using creep test pieces in the uniaxial tension mode in order to grasp the essential basic creep deformation behavior of the bulk material, and the limitation process of creep deformation was studied.

### 2. Experimental

#### 2.1 Test material

Two types of lead-free solders, Sn-3.5Ag and Sn-5Sb were used in this experiment. The chemical compositions of each solders are shown in **Table 1**. The test specimen was prepared as follows. First, the solder bar was melted in an electric furnace heated up to about 623 K in an aluminum crucible, and then poured in a mold made of SUS steel to create a round bar of 14 mm in diameter and 160 mm in length. Here, we set the slope angle of the mold to be 30°.

Next, the solder rods were machined into test specimens measuring 3 mm in diameter and 15 mm in length. All specimens were heat-treated at 333 K for 24 h to remove residual stress and defects induced during specimen forming.

#### 2.2 Creep test method

Creep tests were performed by step test method of increasing creep stresses. First, we performed a creep test under predetermined temperature and creep stress until obtaining steady state creep region. After calculating a steady state creep rate, the creep stress was removed by unloading. In the case of not distinguishing a steady state creep region, we used the minimum creep rate instead of calculating a steady state creep rate.

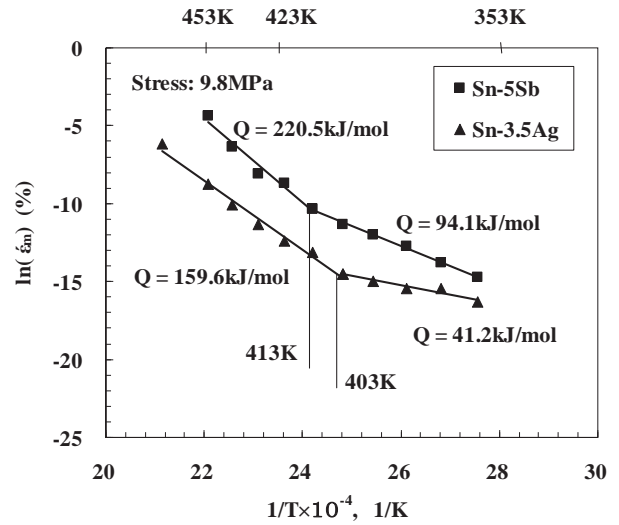
Second, after maintaining it not to take loading for about 2 h, creep test was performed in order to obtain the steady state creep rate by loading again. We carried out the above repeatedly in the applied stress range from 2 MPa to 18 MPa. Raising the test temperature by 10 K, creep tests were performed at temperatures range from 353 K to 453 K. Moreover, raising the applied stress by 1 MPa, we obtained a steady state creep rate or minimum creep rate in the applied stress range from 2 MPa to 18 MPa.

**Table 1** Chemical compositions of the solder alloy

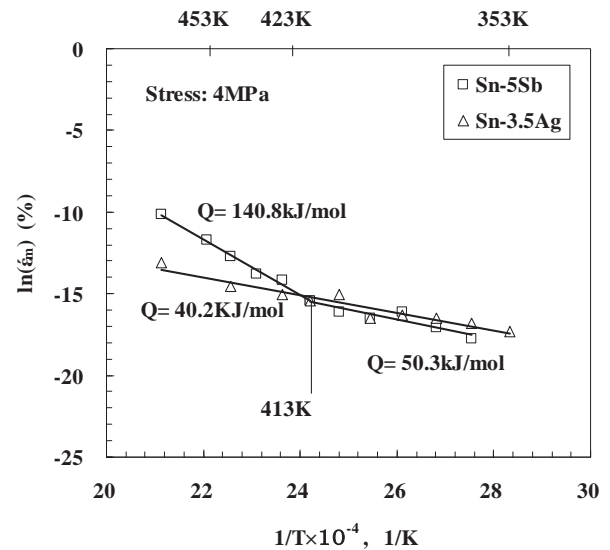
Alloy item	(mass%)					
	Sn	Ag	Sb	Pb	Bi	Fe
Sn-3.5Ag	Bal.	3.47	0.011	0.023	0.002	0.002
Sn-5Sb	Bal.	—	5.09	0.022	0.007	0.001

#### 2.3 Microstructural examination

The samples were prepared for scanning electron microscopy (SEM) by wet grinding to #2000 grit sandpaper, followed by diamond particle polishing down to 0.25 μm and a final polishing stage with a colloidal silica suspension. After polishing, samples were etched by Ar<sup>+</sup> ion milling (GATAN 600) from 30 h to 35 h and then observed via SEM (Hitachi S 4300). We performed microstructural analyses of initial and creep-tested samples with TEM (Hitachi H-9000UHR I) at an accelerating voltage of 300 kV.



(a) Stress at 9.8 MPa



(b) Stress at 4.0 MPa

**Fig. 1** Arrhenius plots of strain and temperature for the Sn-3.5Ag and Sn-5Sb solder alloys under the stress of (a)9.8 MPa, and (b)4.0 MPa.

### 3. Results

#### 3.1 Temperature dependence of creep deformation behavior

The temperature dependence of the minimum creep rate can be described by an Arrhenius-type relational equation, as shown in Eq. (1).

$$\dot{\epsilon}_m = A (\sigma / G)^n \exp(-Q/RT) \quad (1)$$

where,  $A$  is a constant,  $\sigma$  is applied stress,  $G$  is the modulus of rigidity,  $n$  is a stress index,  $R$  is the gas constant, and  $Q$  is apparent activation energy of creep deformation. From Eq. (1), the apparent activation energy for creep deformation  $Q$  can be obtained from the relationship of the natural logarithm of the creep rate and absolute temperature (Arrhenius plot).

The relationship between temperature and the creep deformation rates of the Sn-3.5Ag alloy and Sn-5Sb alloy are shown in **Figure 1**, where the slopes of the lines correspond to the apparent activation energy of creep deformation. From **Fig. 1(a)**, inflection temperature can be seen in the linear sections of the Arrhenius plots of both alloys when the applied stress is 9.8 MPa. Specifically, the creep deformation rates of the alloys increase rapidly when the temperature exceeds 413 K in the Sn-5Sb alloy and 403 K in the Sn-3.5Ag alloy. This inflection temperature corresponds to 0.82 of the melting point of both alloys (505 K in the Sn-5Sb alloy and 494 K in the Sn-3.5Ag alloy, respectively).

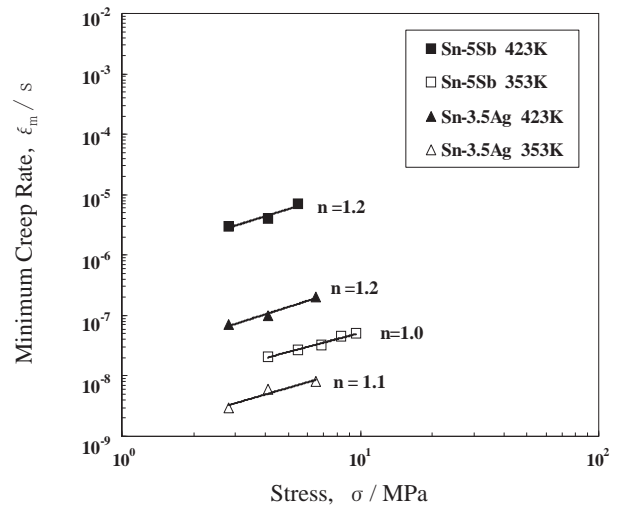
Above this temperature the apparent activation energies of creep deformation of the Sn-5Sb alloy and Sn-3.5Ag alloy also become large, at 220 kJ/mol and 159 kJ/mol, respectively. The fact that the alloys have this large activation energy suggests that recrystallization is activated by lattice (self) diffusion in the microstructure. On the other hand, in the temperature region below the inflection temperature, the apparent activation energy of creep deformation of the Sn-5Sb alloy is 94 kJ/mol, which is close to the value for lattice diffusion (102 kJ/mol) in pure Sn<sup>(6,7)</sup>. Accordingly, the main limitation process for creep deformation is considered to be lattice diffusion.

In contrast to this, the apparent activation energy of creep deformation for the Sn-3.5Ag alloy in the low temperature region is 41 kJ/mol, which is less than a half of the activation energy of lattice diffusion for Sn<sup>(6,7)</sup>. For this reason, the main limitation process for creep deformation is thought to be short path diffusion, like that seen in dislocation core diffusion<sup>7-11)</sup>.

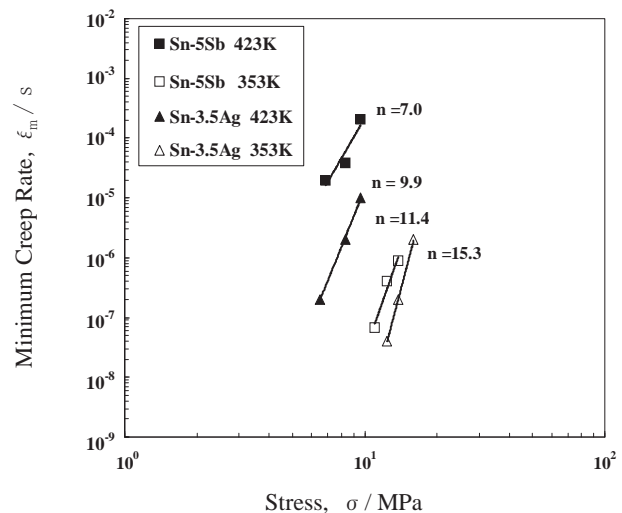
From **Fig. 1(b)**, when the applied stress is 4 MPa, the inflection point for the Sn-5Sb alloy is still around 413 K, but no inflection point can be seen for Sn-3.5Ag. Based on these facts, it can be said that the creep resistance of the Sn-3.5Ag alloy in the low stress region is superior up to high temperatures. This conclusion is in agreement with the previous literature<sup>12)</sup>.

#### 3.2 Stress dependence of creep deformation characteristics

The relationship between applied stress and the minimum creep rate of the two alloys is shown in **Figure 2**, where the slopes of the lines correspond to the stress index  $n$ . When applied stress is in the low stress region (below 6 MPa), the  $n$  values are approximately 1, and do not depend on the temperatures of 353 K and 423 K. Therefore, the limitation process for creep deformation is mainly lattice diffusion or partially grain boundary diffusion, and degradation is mainly controlled by thermal diffusion. On the other hand, the  $n$  value is 7 or more when the applied stress exceeds 6 MPa, and increases with higher stresses over 10 MPa. In this case, it can be thought that creep deformation is mainly limited by dislocation slip, whereas degradation is mainly controlled by applied stress.



(a) Low stress regime ( $\sigma \leq 6$  MPa)



(b) High stress regime ( $\sigma > 6$  MPa)

**Fig. 2** Relationship between the stress  $\sigma$  and minimum creep rate of the Sn-3.5Ag and the Sn-5Sb solder alloys. (a)  $\sigma \leq 6$  MPa, (b)  $\sigma > 6$  MPa.

## High Temperature Creep Properties of Sn-3.5Ag and Sn-5Sb Lead-free Solder Alloys

### 3.3 Relationship between creep characteristics and microstructure

The microscopic structures of the Sn-3.5Ag and Sn-5Sb solder alloys were observed in order to reveal the mechanism of creep deformation described above. The initial stage of microstructures before creep test for Sn-5Sb and Sn-3.5Ag alloys are shown in **Figure 3**. From **Fig. 3(a)**, the existence of a large number of crystal grains having unclear grain boundaries with many undulations was observed in the Sn-3.5Ag alloy.

From the SEM image in **Fig. 3(b)**, it can be understood that the phase composition of the Sn-3.5Ag alloy comprises the primary crystal  $\beta$ -Sn phase (black parts in **Fig. 3(b)**) and an eutectic structure (white contrast) consisting of an  $\text{Ag}_3\text{Sn}$  phase and  $\beta$ -Sn phase. On the other hand, from **Fig. 3(c)**, the Sn-5Sb alloy displays straight grain boundaries and clear contrast of

crystal grains, and the grain size is approximately a few times larger than that of the Sn-3.5Ag alloy. From **Fig. 3(d)**, the larger part of the phase composition of the Sn-5Sb alloy is a  $\beta$ -Sn single phase, and no SnSb system precipitates can be confirmed.

The microscopic structures of the two solder alloys after the creep test are shown in **Figure 4**. In the creep test at a stress of 9.8 MPa, in which the temperature changed from 353 K to 453 K, coarsening of crystal grains and growth of recrystallized grains can be observed in both alloys. Furthermore, in the Sn-5Sb alloy, the grain boundaries change to a complex shape with elongation of the crystal grains in the direction of tensile stress, suggesting that a considerable degree of grain boundary migration occurred accompanying creep deformation in grains.

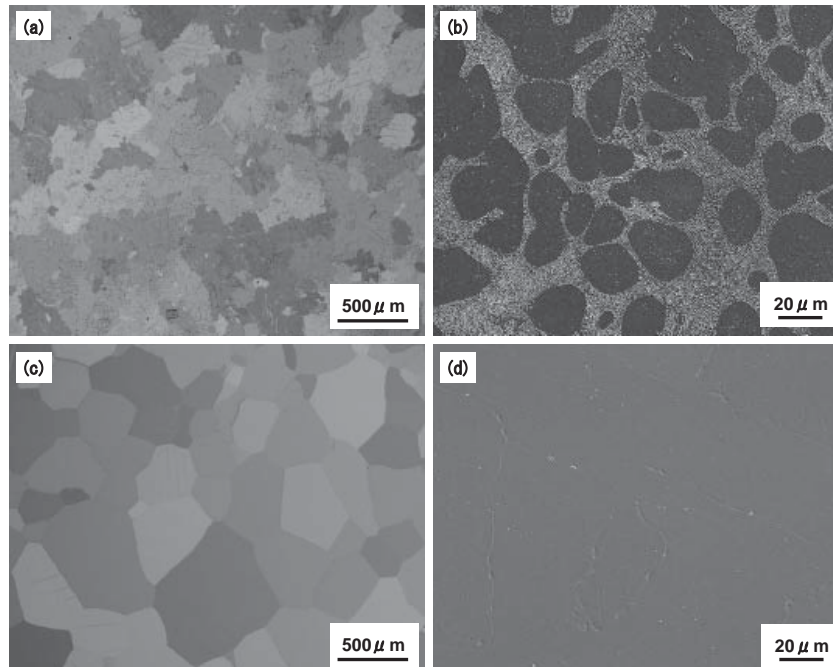


**Fig. 3** Initial stage of microstructures before creep test for Sn-5Sb and Sn-3.5Ag alloys. (a)polarized image of Sn-3.5Ag, (b)SEM image of Sn-3.5Ag, (c)polarized image of Sn-5Sb, (d)SEM image of Sn-5Sb.

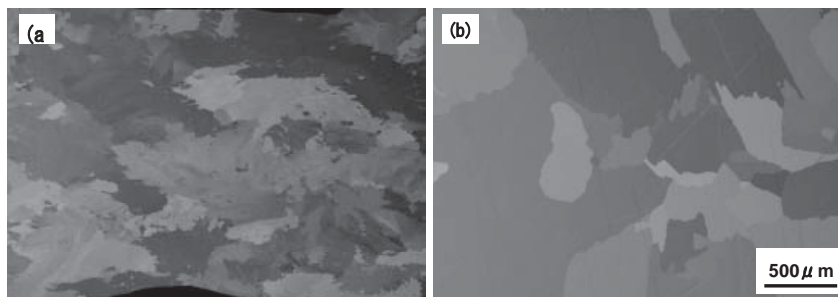


**Fig. 4** Polarized image of microstructure for (a)Sn-3.5 Ag alloy, (b)Sn-5Sb alloy after creep test under 9.8 MPa from 353 K to 453 K. (Stress axis is horizontal)

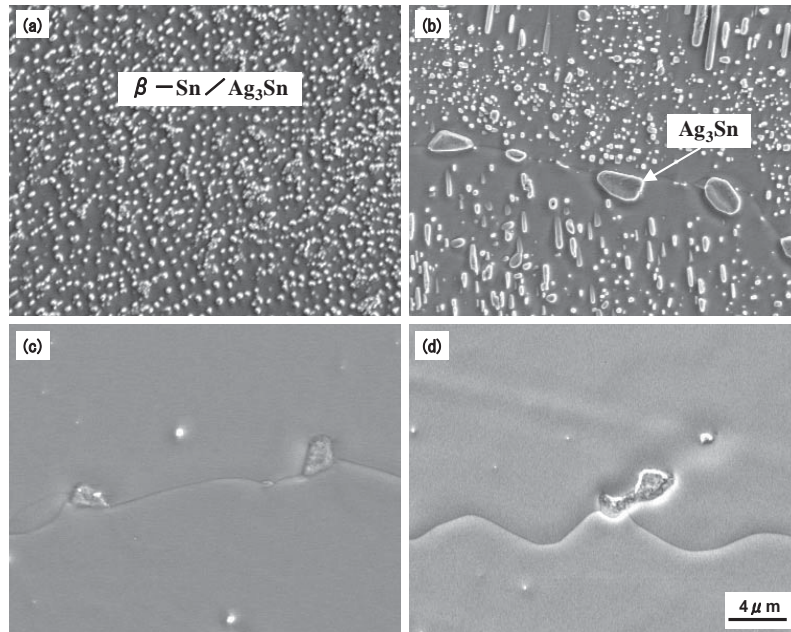


**Fig. 5** SEM photograph of (a) Sn-3.5Ag alloy at initial stage, (b) Sn-3.5Ag alloy after creep test, (c) Sn-5Sb alloy at initial stage, (d) Sn-5Sb alloy after creep test.

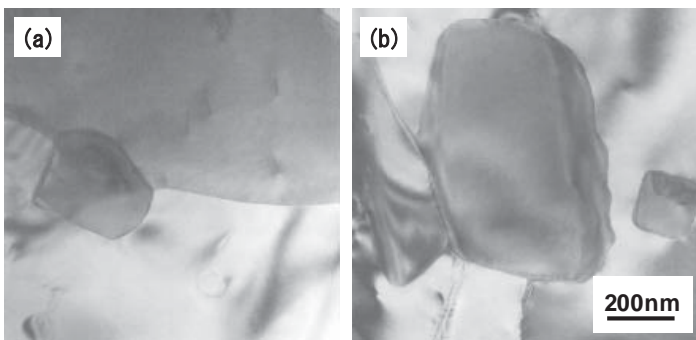


**Fig. 6** TEM photograph of Sn-3.5Ag alloy. (a) initial stage, (b) after creep test under 9.8 MPa, from 353 K to 453 K.

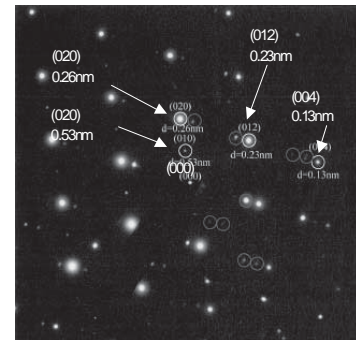


**Fig. 7** Electron diffraction pattern of the  $\text{Ag}_3\text{Sn}$  particles of D part in Fig. 6(b).

**Figure 5** shows SEM images of the initial microstructures of the two alloys and the microstructures after the creep test at stress of 9.8 MPa when the temperature was changed from 353 K to 453 K. From **Fig. 5(a)**, in the initial state, the Sn-3.5Ag alloy displays densely dispersed eutectic microstructures comprising  $\text{Ag}_3\text{Sn}/\beta\text{-Sn}$ . In contrast, after the creep test as shown in **Fig. 5(b)**, the fine eutectic microstructures have grown, and the space between the precipitates has also increased accompanying coarsening of these eutectic microstructures. In addition, aggregation and coarsening of  $\text{Ag}_3\text{Sn}$  has also occurred at the grain boundaries.

On the other hand, in the case of the Sn-5Sb alloy, from **Fig. 5(c)** and **Fig. 5(d)**, only a very slight amount of precipitates, which are considered to be SnSb, can be observed in the grain boundary region from the initial state until completion of the high temperature creep test, and it can be understood that all Sb has dissolved in solid solution in the  $\beta\text{-Sn}$  matrix phase. From these results, it can be thought that the creep deformation resistance of the Sn-3.5Ag alloy increases because the boundary

between fine particles of the eutectic structure and the primary crystal  $\beta\text{-Sn}$  phase does not become a weakening factor, and increased resistance to grain boundary slip can be expected as a result of the fine particles at the grain boundaries, as shown in **Fig. 5(a)** and **Fig. 5(b)**. We also attempted a detailed analysis of the precipitates using a transmission electron microscope (TEM) in order to elucidate the relationship between the precipitates and creep deformation behavior.

**Figure 6** shows TEM images of the Sn-3.5Ag alloy in the initial state and after the creep test at stress of 9.8 MPa. From **Fig. 6(a)**, the size of the particles which crystallized in the initial state was from 0.1  $\mu\text{m}$  to 0.2  $\mu\text{m}$ . However, after the creep test as shown in **Fig. 6(b)**, the size of the particles had grown to more than 0.5  $\mu\text{m}$ , and as a result, it is thought that the effect of these particles in suppressing migration of dislocations was reduced, allowing creep to occur more easily. **Figure 7** shows the electron diffraction pattern of the particles after the creep test at stress of 9.8 MPa. From this diffraction pattern, the particles were confirmed to be the  $\text{Ag}_3\text{Sn}$ .

## High Temperature Creep Properties of Sn-3.5Ag and Sn-5Sb Lead-free Solder Alloys

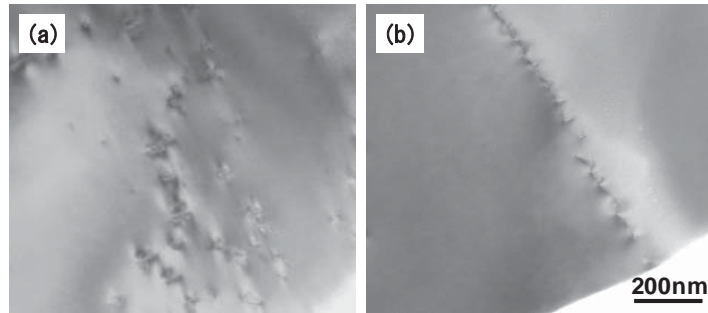


**Fig. 8** TEM photograph of Sn-5Sb alloy. (a)initial stage, (b)after creep test under 9.8 MPa from 353 K to 453 K.

**Figure 8** shows TEM images of the Sn-5Sb alloy in the initial state and after the creep test at stress of 9.8 MPa when the temperature was changed from 353 K to 453 K. In the case of the Sn-5Sb alloy, very few precipitates were observed, as Sb has dissolved in the Sn matrix. Due to the small content of fine precipitates, the creep deformation suppressing effect such as precipitation strengthening is considered to be small.

### 4. Conclusions

The temperature dependence and stress dependence of high temperature creep in Sn-3.5Ag solder alloy and Sn-5Sb solder alloy were investigated by creep tests in order to grasp the essential basic creep deformation behavior of the bulk materials. The findings in this paper are shown as follows.

- (1) From the temperature dependence of the minimum creep rate when the applied stress is 9.8 MPa, the inflection temperature corresponds to 0.82 of the melting point of alloys (494 K). In the temperature region below the inflection temperature, the apparent activation energy of creep deformation of the Sn-3.5Ag alloy is small. Accordingly, the main limitation process for creep deformation is considered to be dislocation core diffusion.
- (2) Above the inflection temperature, the apparent activation energies of creep deformation of the Sn-3.5Ag alloy become large at 159 kJ/mol. Accordingly, the main limitation process for creep deformation is considered to be lattice diffusion.
- (3) From the temperature dependence of the minimum creep rate when the applied stress is below 4 MPa, no inflection point can be seen for Sn-3.5Ag and the apparent activation energy of creep deformation is small. We suspect that the main limitation process for creep deformation can be considered to be grain boundary diffusion.
- (4) The apparent activation energies of creep deformation of the Sn-5Sb alloy have the inflection temperature which corresponds to 0.82 of the melting point of alloys (505 K) when the applied stress is from 4 MPa to 9.8 MPa.
- (5) When the applied stress exceeds 9.8 MPa, the apparent activation energy of creep deformation of the Sn-5Sb alloy is large and the fact that the alloys have this large activation energy suggests

recrystallization is activated by lattice (self) diffusion in the material microstructure.

- (6) In the applied stress of 4 MPa, the main limitation process for creep deformation is considered to be lattice diffusion above the inflection temperature. On the other hand, the main limitation process for creep deformation is considered to be grain boundary diffusion below the inflection temperature.
- (7) In the temperature region from 353 K to 423 K, the stress index  $n$  is approximately 1 when applied stress is in the low stress region not exceeding 6 MPa. Therefore, the limitation process for creep deformation is mainly considered to be lattice diffusion or partially grain boundary diffusion. On the other hand, the  $n$  value is 7 or more when the applied stress exceeds 6 MPa. Therefore, it can be thought that creep deformation is mainly limited by dislocation slip.

### References

- 1) M. Nagano, N. Hidaka, M. Shimoda and H. Watanabe; Proc. of PSEA04, 2004, pp.256-261.
- 2) I. Shohji, H. Watanabe, T. Okashita, and T. Osawa; Mater. Trans., 49-7 (2008) pp.1513-1517.
- 3) M. Nagano, N. Hidaka, M. Shimoda and M. Ono; Journal of Japan Institute of Electronics Packaging, 8-6 (2005) pp.495-501.
- 4) N. Hidaka, M. Nagano, M. Shimoda and H. Watanabe; 11th Symposium on Microjoining and Assembly Technology in Electronics, 11 (2005) pp.171-176.
- 5) T. Nishiyama, H. Kohketsu, K. Takahashi, T. Ogawa and T. Ohsawa; Journal of Japan Institute of Electronics Packaging, 9-3 (2006) pp.162-170.
- 6) D. Shangguan; Lead-Free Solder Interconnect Reliability, ASM, 1995, pp.89.
- 7) Y. Kariya, M. Otsuka, and W. J. Plumbridge; J. Electron. Mater., 32-12 (2003) pp.1398-1402.
- 8) R. J. McCabe and M. E. Fine; Meta.Mate.Trans., 33A (2002) pp.1531-1538.
- 9) Z. Chen, Y. W. Shi and Z.Xia; J. Electron. Mater., 33-9 (2004) pp.964-971.
- 10) C. M. L. Wu and M. L. Huang; J. Electron. Mater., 31-5 (2002) pp.442-448.
- 11) K. Atsumi, Y. Kariya and M. Otsuka; 6th Symposium on Microjoining and Assembly Technology in Electronics, 6 (2000) pp.281-286.
- 12) R. J. McCabe and M. E. Fine; J. Electron. Mater., 31-11 (2002) pp.1276-1282.